Laser-assisted plasma coating at atmospheric pressure: production of yttria-stabilized zirconia thermal barriers

2011 J. Phys. D: Appl. Phys. 44 265202

(http://iopscience.iop.org/0022-3727/44/26/265202)

IOP PUBLISHING JOURNAL OF PHYSICS D: APPLIED PHYSICS

J. Phys. D: Appl. Phys. **44** (2011) 265202 (5pp) doi:10.1088/0022-3727/44/26/265202

Laser-assisted plasma coating at atmospheric pressure: production of yttria-stabilized zirconia thermal barriers

Zihao Ouyang, Liang Meng, Priya Raman, Tae S Cho and D N Ruzic

Center for Plasma Material Interactions, Department of Nuclear Plasma and Radiological Engineering, University of Illinois at Urbana-Champaign, Urbana, IL 61801, USA

E-mail: tscho@illinois.edu

Received 19 March 2011, in final form 25 May 2011
Published 13 June 2011
Online at stacks.iop.org/JPhysD/44/265202

Abstract

A laser-assisted plasma-coating technique at atmospheric pressure (LAPCAP) has been investigated. The electron temperature, electron density and gas temperature of the atmospheric-pressure plasma have been measured using optical emission spectroscopy (OES). LAPCAP utilizes laser ablation of 3 mol% yttria-stabilized zirconia into an atmospheric helium/nitrogen plasma to deposit thermal barrier coatings on a nickel-based substrate. The deposited film shows columnar structures similar to films prepared by high-vacuum deposition methods, such as physical vapour deposition and conventional pulsed-laser deposition. However, the LAPCAP films have smaller columns and higher porosity, compared with the films deposited by other techniques. The morphology and characteristics of the films have been analysed by scanning electron microscope, focused ion beam and x-ray diffraction.

(Some figures in this article are in colour only in the electronic version)

Introduction

Thermal barrier coatings (TBCs) have been widely used in aerospace-related, mechanical and electro-chemical components and systems because of their capabilities of lowering metal surface temperatures and protecting thermal oxidation in high-temperature operations [1]. To improve the operation efficiency of practical applications, it is indispensable for TBCs to maintain high stability and adhesion when they are subjected to considerable gas turbulence and heat corrosion. The performance requirements of TBCs under extreme operating conditions motivate the search for suitable materials and process methods to achieve the desired parameters.

Yttria-stabilized zirconia (YSZ) is one of the most common TBC materials for its desirable properties: high melting point (2600–2700 °C), low thermal conductivity ($\sim$2.0 W m^{-1} K^{-1} at 1100 °C) and high thermal expansion coefficient (10.1 $\times$ 10^{-6} K^{-1} at 600 °C) [2, 3]. Additionally, when YSZ intermolecular bonds are broken, bonds with a higher atomic packing factor (APF) will be formed to make the YSZ fracture resistant. Previous research has shown that the porosity of YSZ thin films and other TBCs determines the mechanical and thermal performance. Porosity-free TBC films have lower ohmic resistances, while high-porosity films have much lower thermal conductivities [4].

YSZ TBCs deposited by traditional air plasma spraying (APS) technique is accomplished by adding nanoscale YSZ powder with a grain size of 25–500 nm into a high-temperature air plasma plume. APS is a cost-effective technique with high deposition rate, but the deposited films are physically interlocked with the substrate, which usually have a highly molten lamella microstructure with micro-pores and micro-cracks presented in the films [5].

Other deposition methods, such as electron beam-physical vapour deposition (EB-PVD) and pulsed-laser deposition (PLD), are employed to grow fully dense or porous columnar-structured YSZ films which have strong chemical adhesion and lower erosion rate than lamellar structure TBCs [6]. The deposition is typically performed at the temperatures of 600 °C–900 °C and pressures of 10^{-3}–10^{-1} Torr in oxygen environment [7–9]. EB-PVD and PLD have relatively small deposition rates compared with APS, and also require an expensive vacuum chamber, heating system and laser device,

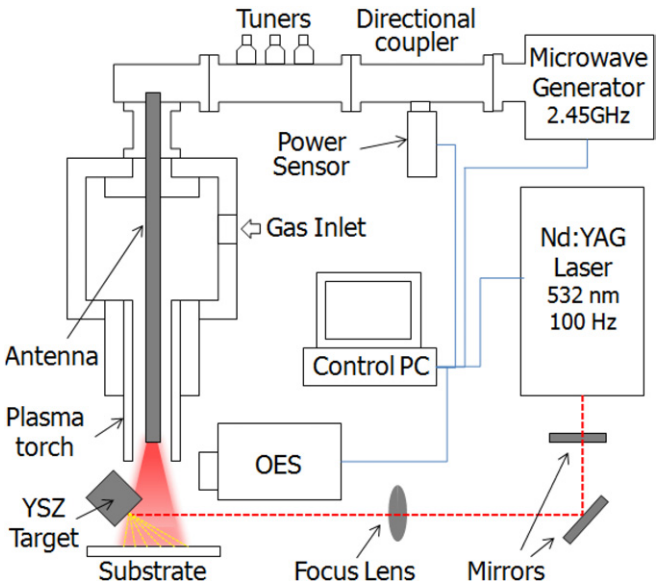

Figure 1. Schematic diagram of YSZ deposition by laser-assisted plasma coating at atmospheric pressure (LAPCAP).

but they are able to control the deposition profile by simply adjusting the parameters and orientations of the parts in the system to achieve dense or porous columnar structures.

In this study, laser-assisted plasma coating at atmospheric pressure (LAPCAP) has been investigated for the first time to produce columnar-structured YSZ film. The basic concept of LAPCAP is to use a laser to ablate YSZ into an atmospheric-pressure plasma plume. The atmospheric plasma heats the substrate and entrains the laser-ablated species allowing a high-percentage of the atoms to reach the substrate. Since it is an atomic flux that reaches the substrate, the microstructure of the deposited coatings can be improved. This technique does not require vacuum systems and nor does it require additional heat sources for the target and substrate, and it has many other favourable advantages, such as high deposition rate and good compliance for automated control.

1. Experimental

The atmospheric-pressure plasma source was ignited in a plasma torch by a 2.45 GHz microwave generator, as shown in figure 1. The microwave generator had a maximum output power of 6 kW, and the reflected power was kept below 5% of output power in all experiments. The plasma torch consists of three copper hollow cylinders, a copper antenna at the centre and a quartz discharge tube which had an inside diameter of 13 mm. A mixture of helium and nitrogen was used to generate a large-volume, high-temperature plasma plume. The largest plasma plume was created using a He (99%) + N_2 (1%) mixture gas, which also resulted in the highest plasma gas temperature at a given output microwave power. The target used in this study was cylinder-shaped 3 mol% yittra (Y_2O_3) stabilized zirconia (ZrO_2) (YSZ) which had a 10 mm diameter and a 10 mm height. The target was mounted on a motor, which is rotating at 2 rpm, and the substrate was positioned ∼1 cm away from the exit of the plasma torch, as shown

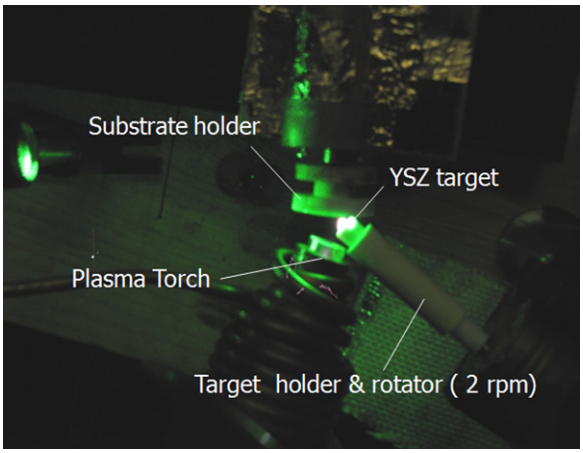

Figure 2. Operation of YSZ deposition systems of laser-assisted plasma coating at atmospheric pressure.

in figures 1 and 2. For comparison purposes, two kinds of film were prepared by PLD and LAPCAP. The PLD film was prepared at atmosphere pressure in air and the LAPCAP film was prepared by He/N_2 atmospheric-pressure plasma assisted laser ablation. The substrate was heated up to ∼800 °C by the plasma during LAPCAP process. The target–substrate distance was approximately 1 mm for both cases. The substrate used in this work was a nickel-based single-crystal René N5 super-alloy. A 50 μm platinum–aluminide bond coat has been deposited on the substrate in order to increase the adhesion.

A Nd : YAG laser (Spectra-Physics; 532 nm wavelength, 8–12 ns pulse width) with 100 Hz pulse repetition rate and 120 mJ/pulse was focused by a UV fused silica lens to ablate the target, yielding an ablation energy density of ∼10 J cm^{-2}. The YSZ target was immersed in the plasma plume in order to melt the possible micro-sized fragments escaping from the target during the ablation. An optical emission spectroscopy (OES) system was used to measure the electron temperature, electron density and gas temperature. The OES system consists of a 0.275 meter focal length monochromator (Acton Research Corporation, Model SpectraPro® 275), a spectrometer sensor engine (SSE) (Mightex Systems), an optical fibre and focus lenses. The monochromator has a resolution of 0.05 nm with a 2400 g mm^{-1} grating.

The deposition rate of YSZ film with LAPCAP was approximately 1–2 μm min^{-1}. The film thicknesses were less than 10 μm. The morphologies of the YSZ films prepared with PLD and LACAP were compared by means of scanning electron microscopy (SEM: Hitachi S-4800), focused ion beam (FIB: FEI Dual Beam 235 FIB) and x-ray diffraction (XRD: Philips X'pert).

2. Plasma diagnostics

OES was used to measure the electron temperature (T_e), electron density (n_e) and plasma gas temperature (T_g). OES is believed to be reliable in high-pressure plasma discharges, because the atoms, ions and electrons can be considered to be in local thermodynamic equilibrium. In this study, the degree of ionization is large enough such that abundant free electrons allow the density distribution of excited atomic

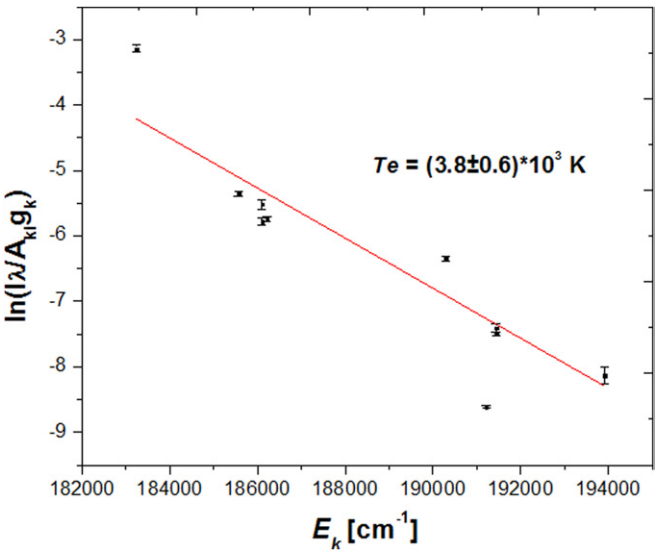

Figure 3. The line corresponds to the best linear fitting where estimated T_e is 3800 K.

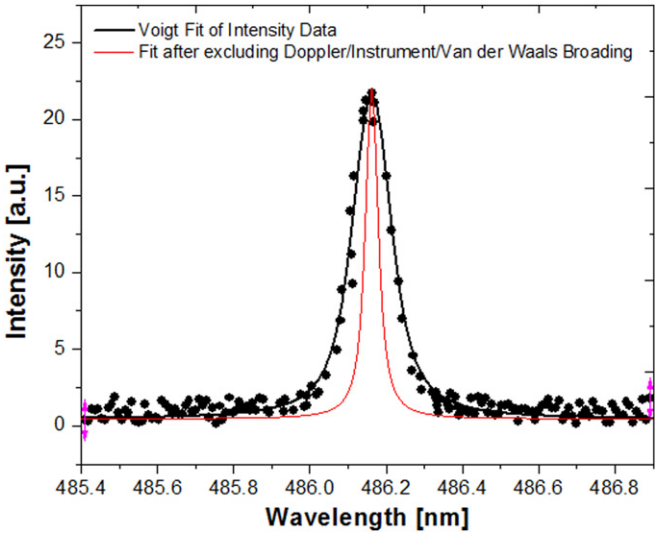

Figure 4. Experimental H_β profile (spectrum is taken at the deposition spot). Red line shows the Voigt fit for the experimental data. Blue line shows the fit after excluding the instrumental, Doppler and van der Waals broadenings, which is approximately the profile of the Stark broadening.

states to be a Boltzmann distribution. Therefore the relation between the spectral intensity and the energy of an excited state satisfies [10]

$$\frac{\ln(I_{p\to k}\lambda_{p\to k})}{g(p)A_{p\to k}} = -\frac{E(p)}{kT_e} + \text{constant}, \qquad (1)$$

where $I_{p\to k}$, $\lambda_{p\to k}$ and $A_{p\to k}$ are the relative intensity, peak wavelength and the Einstein constant for spontaneous emission of a specific spectral line representing a transition $p \to k$, and $g(p)$ and $E(p)$ are the statistical weights and photon energy of excited state p, respectively. The reference data of $\lambda_{p\to k}$, $A_{p\to k}$, $g(p)$ and $E(p)$ for a particular transition can be found at NIST Atomic Spectra Database. In this study, the relative intensity of multiple transitions of the helium plasma were measured, therefore, T_e could be determined by the slope on the plot of $\ln(I_{p\to k}\lambda_{p\to k})/g(p)A_{p\to k}$ versus $E(p)$, which is known as the Boltzmann plot, as shown in figure 3. The measured T_e is 3800 ± 600 K (∼0.3 eV), which is a typical value for this type of atmospheric-pressure plasma.

The electron density n_e is calculated using the Stark broadening of the hydrogen Balmer β line (H_β) at 486.1 nm. The full-width at half-maximum (FWHM) of H_β line due to Stark broadening is given by Griem in [11]

$$\Delta\lambda_{stark} = 2.50 \times 10^{-9}\alpha_{1/2}n_e^{3/2}, \qquad (2)$$

where $\Delta\lambda_{Stark}$ is in nm, n_e is in cm^{-3} and $\alpha_{1/2}$ is the reduced wavelength tabulated in [12]. For the H_β line, $\alpha_{1/2}$ is in the range 7.62×10^{-3}–8.03×10^{-3} nm if T_e is from 5000 ∼ 10 000 K and n_e is from 10^{14}–10^{15} cm^{-3}. In this study, $\alpha_{1/2} = 7.83 \times 10^{-3}$ nm is used as an average value.

Three other broadening mechanisms, instrumental broadening, Doppler broadening and Van der Waals broadening, are considered, besides the Stark broadening and contribution of each mechanism for the overall line shape has been determined [11, 13]. Figure 3, the Voigt fit which was taken from an atmospheric-pressure microwave plasma, shows the fit after excluding the instrumental, Doppler and Van der Waals broadenings, which is approximately the profile of the Stark broadening. The shape of the H_β line is shown in figure 4. Contribution of each mechanism for the overall line shape is listed in table 1. The electron density calculated by equation (2) is $(1.98 \pm 0.59) \times 10^{14}$ cm^{-3}.

The N_2 second positive system (C–B) in the range 360–390 nm is used to determine the gas temperature T_g. The rotational temperature is obtained by fitting the measured spectrum with the calculated spectrum by the SPECAIR code [14], which is a good estimate of T_g in atmosphere pressure plasmas. The slit function is chosen to be a triangle of base width 0.35 nm in order to obtain the best fit for the measured N_2 C–B spectrum in the SPECAIR calculation. An example is shown in figure 5, which compares the measured N_2 C–B spectrum (364–383 nm) with the SPECAIR best fit in the atmospheric helium/nitrogen ($He : N_2 = 99 : 1$) plasma at $T_g \approx 1100 \pm 100$ K.

3. Characteristics of the deposited YSZ films

In many applications such as TBCs for turbine blades, one crucial requirement for the films is the columnar structure with proper porosity among the individual columns. Figure 6 shows the SEM images of YSZ film deposited using PLD (a) and LAPCAP (b) at atmospheric pressure. Some micro-sized fragments of 1–5 μm spherical or quasi-spherical clusters are clearly visible for both cases. These fragments might be formed by the agglomeration of the intensified particle ejection from the ablation spot due to the high-fluence nanosecond-laser ablation (∼10 J cm^{-2}). However, the dominant structure of the LAPCAP YSZ film deposited at 800 °C is mostly sub-micrometre filamentous clusters (<500 nm), but the PLD film deposited at 20 °C shows mainly micrometre-sized clusters (1–5 μm). Also, the LAPCAP film has better uniformity and less undesired micro-sized particles,

Table 1. Contributions for the experimental profile from the H_β line.

Voigt (nm)	Gaussian (nm)		Lorentzian (nm)		n_e (cm^{-3})
	$\Delta\lambda_D$	$\Delta\lambda_{Instrument}$	$\Delta\lambda_\alpha$	$\Delta\lambda_{Stark}$	
0.132 ± 0.022	0.006 ± 0.0003	0.039 ± 0.008	0.025 ± 0.002	0.068 ± 0.013	$(1.98 \pm 0.59) \times 10^{14}$

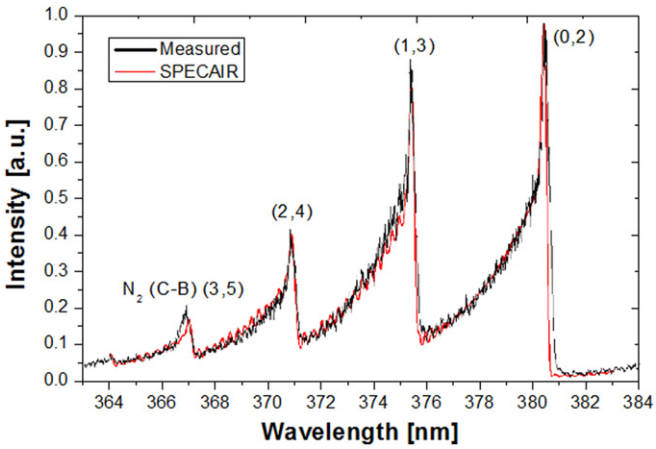

Figure 5. Measured N_2 C–B spectrum (364–383 nm, $\Delta v = -2$) of the helium/nitrogen plasma. SPECAIR best-fit spectrum gives a rotational temperature of 1100 ± 100 K.

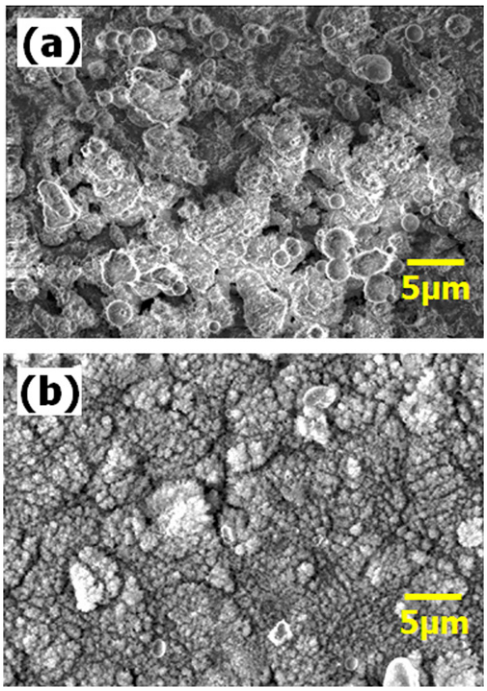

Figure 6. SEM images of YSZ films deposited with PLD (a) and with laser-assisted plasma coating at atmospheric pressure (b).

and the trenches between these small clusters can be clearly distinguished.

FIB has been used to verify the formation of the columnar structure of the films. Figure 7 shows the cross-sectional images of the films deposited with PLD (a), LAPCAP (b) and more magnified images for LAPCAP (c). The columnar structure of the LAPCAP film can be clearly seen in figures 7(b) and (c), whereas the PLD film is relatively porous, and does not have any columnar structure. This result confirms that the

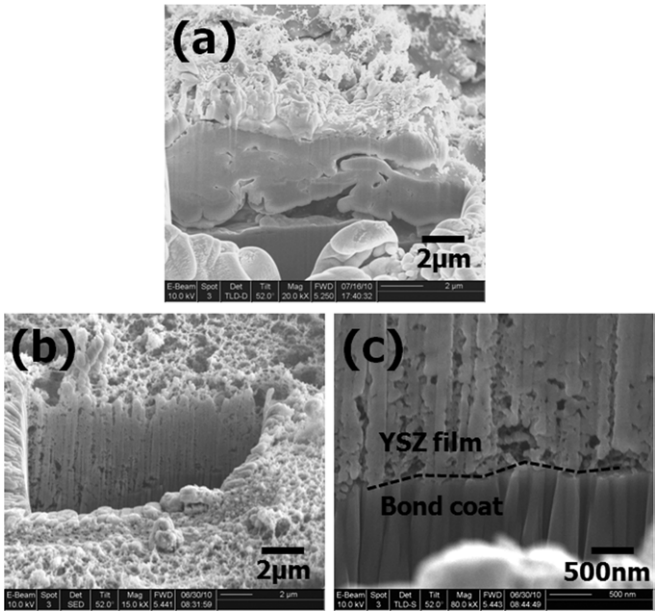

Figure 7. Cross-sectional FIB images of YSZ films deposited with PLD (a) and with laser-assisted plasma coating at atmospheric pressure (b) and more magnified LAPCAP deposition (c).

vaporized particles/atoms generated during the laser ablation process are drastically decelerated by frequent collisions with the molecules in ambient air environment before they arrive at the surface of the substrate. The plasma size produced by the laser ablation at energy density of 10 J cm^{-2} was approximately 1 mm, while LAPCAP had a 1 cm length of the plasma plume. It should be emphasized that in order to obtain adhesive YSZ film, the target–substrate distance was kept less than 3 mm in this study. The assisted helium/nitrogen plasma has the ability of slowing down the thermalization process of the ablated species, thus the quality of the film can be improved at a higher deposition temperature.

The phase composition of the YSZ films using the two different deposition methods was analysed by XRD and compared with the results of the YSZ target itself, as shown in figure 8. It is noted that all the YSZ films were crystallized in a cubic phase. Compared with the YSZ target, several additional peaks can be seen in all the deposited films, such as Ni (1 1 1), which might be originated from the substrate and the bond coat material. Furthermore, it is noticeable that the primary diffraction peak in all films is on the (1 1 1) plane of the YSZ cubic, whereas (1 1 1) and (2 2 0) diffraction peaks are almost equivalent in the YSZ target.

4. Conclusions

A new deposition technique, laser-assisted plasma coating at atmospheric pressure (LAPCAP) has been introduced and

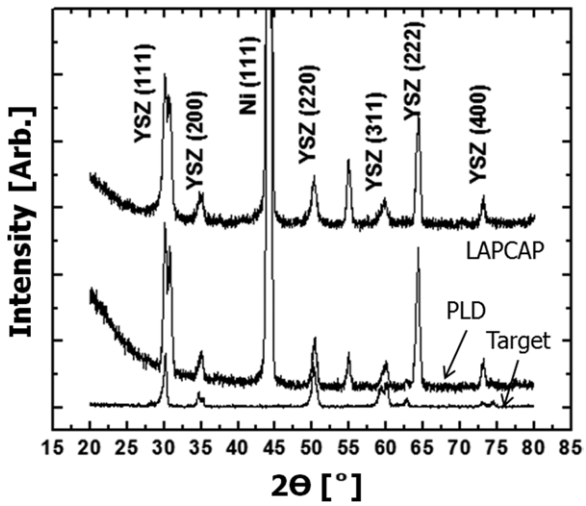

Figure 8. XRD patterns of the YSZ target and the YSZ films deposited with PLD and laser-assisted plasma coating at atmospheric pressure.

successfully applied to TBCs. OES shows that the electron temperature, electron density and gas temperature are 3800 ± 600 K, 10^{14}–10^{15} cm^{-3} and 1100 ± 100 K, respectively.

Columnar-structured YSZ films have been grown on the René N5 substrates at atmospheric pressure using the LAPCAP technique. Microstructures of the films deposited with and without the helium/nitrogen plasma assistance are compared. Films deposited at high deposition temperature of 800 °C by LAPCAP showed good uniformity and distinguished sub-micron columns, whereas films deposited with PLD showed mostly micrometre-sized clusters with high porosity. The XRD results showed that the films were fully stabilized in a cubic phase for both deposition conditions. The assisted atmospheric helium/nitrogen plasma in the LAPCAP configuration has the ability to increase the size of the YSZ evaporation volume induced by the laser ablation. The comparison of the microstructures of the YSZ films deposited by LAPCAP and PLD techniques confirms that the film deposited by LAPCAP has more uniform columns, smaller column size and less porosity than the one deposited by PLD at atmospheric pressure.

References

[1] Singhal S C 2003 *High Temperature Solid Oxide Fuel Cells: Fundamentals, Design and Applications* (Oxford: Elsevier)
[2] Su Y J, Trice R W, Faber K T, Wang H and Porter W D 2004 *Oxid. Met.* **61** 253
[3] Hayashi H, Saitou T, Maruyama N, Inaba H, Kawamura K and Mori M 2005 *Solid State Ion.* **176** 613
[4] Will J, Mitterdorfer A, Kleinlogel C, Perednis D and Gauckler L J 2000 *Solid State Ion.* **131** 79
[5] Berndt C C, Michlik P and Racek O 2004 *Proc. Int. Thermal Spray Conf. (Osaka, Japan)* p 1110
[6] Nicholls J R, Pereira V, Lawson K J and Rickerby D S 1998 *Proc. RTO AVT Workshop on 'Intelligent Processing of High Performance Materials' (Brussels, Belgium)* pp 16-1
[7] Infortuna A, Harvey A S and Gauckler L J 2008 *Adv. Funct. Mater.* **18** 127
[8] Jung Y, Sasaki T, Tomimatsu T, Matsunaga K, Yamamoto T, Kagawa Y and Ikuhara Y 2003 *Sci. Technol. Adv. Mater.* **4** 571
[9] Voevodin A A, Jones J G and Zabinski J S 2000 *J. Appl. Phys.* **88** 1088
[10] Gamero A 1998 *Spectroscopic Diagnostics of High Pressure Discharges J. Phys. IV France* **8** 339
[11] Griem H R 1964 *Plasma Spectroscopy* (New York: McGraw-Hill)
[12] Griem H R 1974 *Spectral Line Broadening by Plasmas* (New York: Academic)
[13] Laux C O, Spence T G, Kruger C H and Zare R N 2003 *Plasma Sources Sci. Technol.* **12** 125
[14] Lauz C O 2002 Radiation and nonequilibrium collisional–radiative models (*von Karmen Institute Lecture Series* 2002-2007) *Physico-Chemical Modeling of High Enthalpy and Plasma Flows* ed D Feltcher *et al* (Belgium: Rhode-Saint-Genèse)